Available online at www.sciencedirect.com
ScienceDirect
Materials Chemistry and Physics 104 (2007) 141–145
MATERIALS CHEMISTRY AND PHYSICS
www.elsevier.com/locate/matchemphys

Fabrication of three-dimensional network of ZnO tetratpods and its response to ethanol

Jean-Jacques Delaunay *, Naoki Kakoiyama, Ichiro Yamada

Department of Eng. Synthesis, School of Engineering, The University of Tokyo, 7-3-1 Hongo Bunkyoku, Tokyo 113-8656, Japan

Received 3 March 2006; received in revised form 22 December 2006; accepted 27 February 2007

Abstract

A three-dimensional network of ZnO tetrapods was fabricated on a quartz substrate. The interconnected tetrapods, having legs with length of several μm and diameter in the 0.1–1 μm range, were synthesized via a simple thermal oxidation reaction. Zn powder was heated in a furnace at a temperature of 900 °C and was made to react with air and water vapor. The content of water vapor in air was found to control the adherence onto the substrate and the morphology of the deposited layers. The layers developed a grain structure or a porous structure made of interconnected tetrapods, depending on the content of water vapor in air. The network of tetrapods which was obtained for a small content of water vapor formed a highly porous layer with a high surface to volume ratio. The tetrapod network was tested as a gas sensing element by measuring changes in its electrical resistance upon exposure to ethanol. The responses to ethanol were investigated as a function of the layer temperature and the ethanol concentration. The optimum temperature of the tetrapod network layer was found to be 400 °C, at which ethanol concentration as low as 0.5 ppm was easily detected. The tetrapod network exhibited a 10-fold increase in sensitivity when compared with a ZnO polycrystalline thick film.

Keywords: Metal oxide semiconductor; ZnO; Nanostructure; Tetrapod; Gas sensor

1. Introduction

ZnO, a II–VI compound semiconductor, has found a multitude of applications as a result of its wide and direct band gap, its high exciton binding energy at room temperature, its ease of fabrication and its good safety record (for a review see, for example [1,2]). Synthesis of ZnO nanostructures [3–6] has revealed more fields in which this material can be utilized. ZnO nanostructures have potential uses in catalysis [7,8], in field electron emission [9], in gas sensing [10,11] and in hydrogen storage [6]. Tetrapods were the first nanostructures of ZnO to be synthesized [3], but it is only recently that their photoluminescence [5] and gas sensing properties [11] have been investigated. Other ZnO nanostructures such as nanorods [4] and nanowires [6,10] have been produced in the form of powder. Investigations into the gas sensing properties of these nanostructures were conducted on thick layers prepared from powder of tetrapods and nanowires [10,11]. The method used in the fabrication of a gas sensing element from nanostructured powder typically consists of the following three steps: (1) ultrasonic dispersion of the ZnO nanostructured powder in a solution (may contain an adhesive), (2) layer deposition by spray or spin coating of the dispersed material, and (3) drying/curing of the resulting layer. In this paper, we report the direct deposition on quartz substrates of thick layers consisting of interconnected tetrapods of ZnO forming a three dimensional network. The crystal structure and morphology of the thick layers are characterized, and the layer electrical responses to ethanol vapor are investigated as a function of the layer temperature.

2. Experimental

Thick ZnO layers were prepared via a thermal oxidation reaction in air from Zn powder (Nilaco, 99.9998% purity) placed in a quartz tube heated in a furnace using the experimental setup depicted in Fig. 1. The furnace temperature was controlled at ±1 °C and had a temperature gradient of 3 °C cm^{-1} at 1000 °C in the heating zone. The furnace temperature was set at 900 °C as it was found in our previous study [12] that the thermal oxidation reaction which starts at a temperature of ≃ 900 °C produces a high yield of nanostructures. The fabrication process did not rely on metal catalysts. In this study, the effects of air flow and its humidity content on the layer morphology are investigated. Four layers were fabricated under the conditions summarized in Table 1. Gas circulation in the furnace quartz tube was obtained either by thermal convection (quartz tube apertures kept open) or by forced convection (quartz tube aperture connected to an

* Corresponding author. Tel.: +81 3 5841 3017; fax: +81 3 5841 8818.
E-mail address: jean@mech.t.u-tokyo.ac.jp (J.-J. Delaunay).

0254-0584/$ – see front matter © 2007 Elsevier B.V. All rights reserved.
doi:10.1016/j.matchemphys.2007.02.099

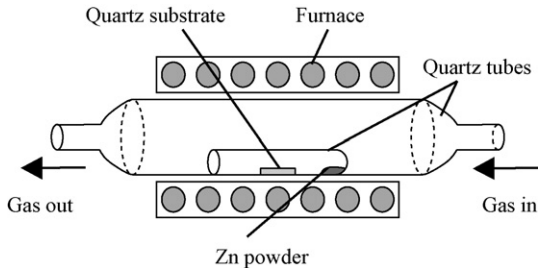

Fig. 1. Schematic of the experimental arrangement for the fabrication of the ZnO layers.

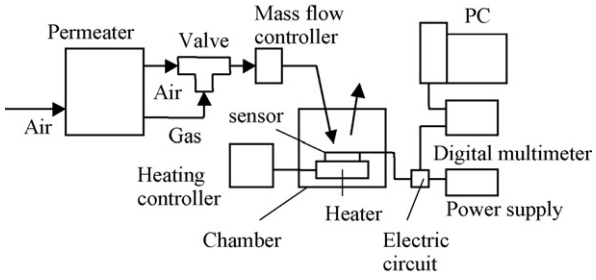

Fig. 2. Schematic of the measurement setup used to record gas responses.

air cylinder through a mass flow controller set at 100 standard cubic centimeters per minute). Humid air was obtained by three means (1) using ambient air, (2) using a humidifier, and (3) bubbling dry air through pure water. The amount of humidity in the circulated air was varied from nearly 0 to about 30 g m^{-3}. The reaction products consisted both of powder deposit and layer deposit. Powder samples obtained using thermal convection under low humidity conditions have been analyzed elsewhere [12]. The four fabricated layers, denoted A, B, C and D, with a texture resembling that of frosted glass diffuser were deposited on quartz substrates and used as sensing element in trace gas detection experiments.

The crystal structure of the fabricated layers was analyzed using X-ray diffraction on a MacScience instrument operating with the Cu Kα radiation and recording θ–2θ scans with a 0.02° resolution on 2θ. The sample morphology was investigated using a Scanning Electron Microscope (SEM Hitachi S2400 operated at an acceleration voltage of 20 kV). The samples were investigated for the presence of impurity with X-ray fluorescence analysis (Horiba, XGT5000). The structural analysis results of our ZnO layers were compared with those of a reference ZnO powder (Koch Chemicals, 99.999% purity).

The gas sensing characteristics of the fabricated ZnO layers deposited on quartz substrates (20 mm × 10 mm) were investigated using the experimental setup of Fig. 2. The variation in resistance of the thick ZnO layers upon exposure to ethanol vapor was recorded as a function of the layer temperature. The resistance of the sensing element was determined using a standard voltage divider circuit in which the sensing element was connected in series to a resistance of 1 MΩ and to a constant voltage source of 10 V. The material of the sensing element was found ohmic in the voltage range used in this study (1–10 V). The

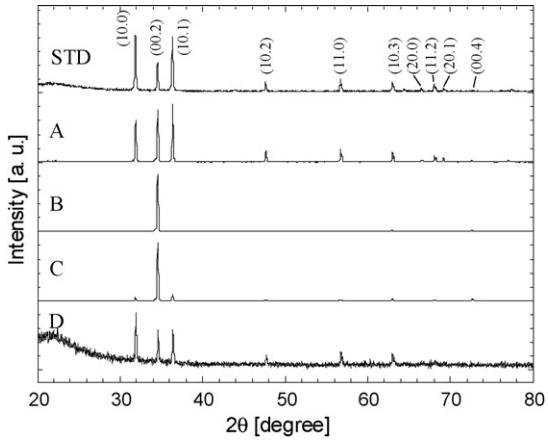

Fig. 3. X-ray diffraction data of fabricated ZnO layers (denoted A, B, C and D in the figure), together with that of the ZnO reference powder (denoted STD).

gas flow was generated by circulating pure air from a cylinder (air purity better than 100 ppb for the total hydrogenated carbon content) into a permeater (Gastec PD-1B-2, double line) containing a diffusion tube with liquid ethanol at a fixed temperature. All experiments used the same constant gas flow of 0.5 L min^{-1}. The gas concentration relative to pure air was controlled by varying the temperature and the size of the diffusion tube which contained the ethanol. The concentration of ethanol in air can be computed using the temperature, the partial pressure of the ethanol vapor, and the diffusion tube dimensions. Ethanol concentration varied in the range of 0.5–50 ppm. The second separate chamber of our double line permeater was used to generate a flow of pure air at the same temperature as that of the flow of ethanol vapor in air. The flow in the flask can be switched from pure air to ethanol vapor in air by using a valve. The flask where the sensing element was tested had a volume of 1 L. The temperature of the sensing element was controlled by a heater for use in vacuum systems, so that degassing from the heater itself was kept to a minimum. The temperature of the heater was calibrated against the temperature of the sensor element. Stainless steel and Teflon, both materials inert to the investigated gas mixtures, were used exclusively in connecting the different elements of the gas sensing setup (air cylinder, pressure regulator, permeater, mass flow controller and flask). Finally, the flask and the heater were baked for half a day prior to gas experiments so as to ensure minimum contamination.

3. Results

X-ray diffraction data for the four samples and the reference powder are shown in Fig. 3. The observed peaks of the reference ZnO powder sample could be indexed to the hexagonal wurtzite structure of the ZnO, with cell parameters of $a = 3.249$ Å and $c = 5.207$ Å [13]. Samples A and D exhibited very similar diffraction data to that of the reference powder sample, strongly

Table 1
Fabrication conditions of the ZnO samples

	Sample			
	A	B	C	D
Furnace temperature	900 °C			
Gas flow	Natural convection		100 sccm	
Water content	∼5 g m^{-3} (ambient air)	∼30 g m^{-3} (humidifier)	∼10 g m^{-3} (bubbling in water)	0 g m^{-3} (pure air)
Reaction time	30 min			
Process repetition	3	3	1	3

The masses of water vapor per unit volume of air computed from the measurements of air temperature and air relative humidity are given as estimates. For layers A and B, the deposition process was repeated so as to obtain a sheet resistance at room temperature less than 100 MΩ. For sample D, poor adherence on the quartz substrate was observed.

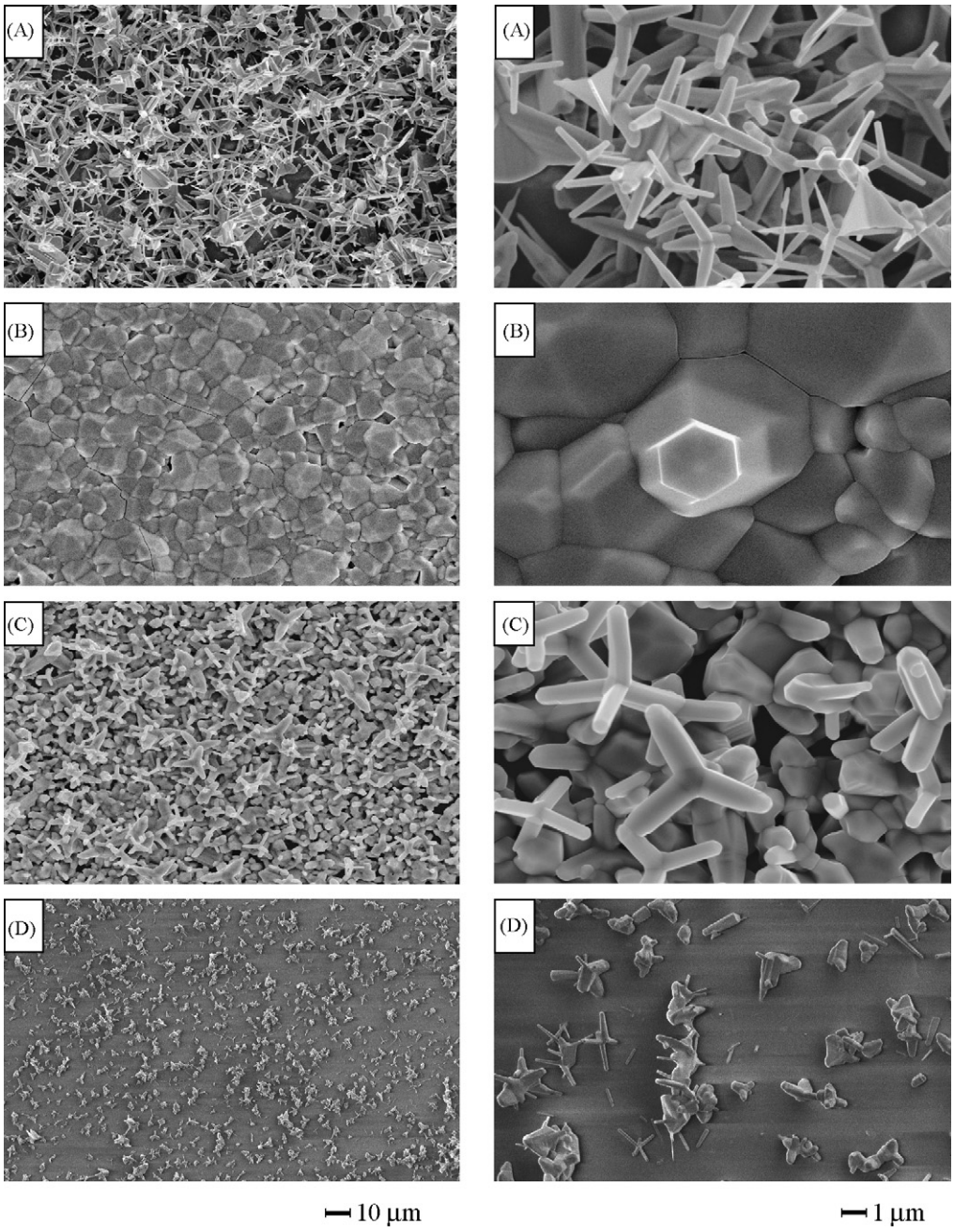

Fig. 4. Low magnification (left) and high magnification (right) SEM images of the ZnO samples A, B, C, and D. SEM observations were conducted without a conductive layer for all samples (FE-SEM was used for sample D).

indicating that these samples were in the wurtzite structure. The relative intensities of the diffraction peaks of samples A and D were in fair agreement with those tabulated in standard powder diffraction data [14], indicating that these samples consisted of nearly randomly oriented crystals of good quality. For samples B and C, the predominant intensity of the (00.2) peak is evidence for a preferred growth of the ZnO crystals in the crystallographic *c*-axis direction, a characteristic commonly found in the growth of thick ZnO films and attributed to a higher growth rate in that direction (see, for example [15,16]).

XFA analysis of our samples revealed no metallic impurities above the detection limit (∼0.01 at.% level), which confirmed that our layers were synthesized without metallic catalysts. Note that a self-catalyst mechanism in the growth of ZnO nanostructures by thermal oxidation of Zn may be at play [9].

The SEM images of Fig. 4 revealed different morphologies for samples A, B, C, and D. Sample A consisted mainly of interconnected tetrapods having legs with length of several μm and diameter in the 0.1–1 μm range. A few microplates were also observed in sample A. Sample B showed a typical grain structure of polycrystalline thick films, with grain size in the 1–10 μm range. A close inspection of the surface of sample B revealed cracks, which were very likely developed during the sample cooling due to the difference in thermal expansion

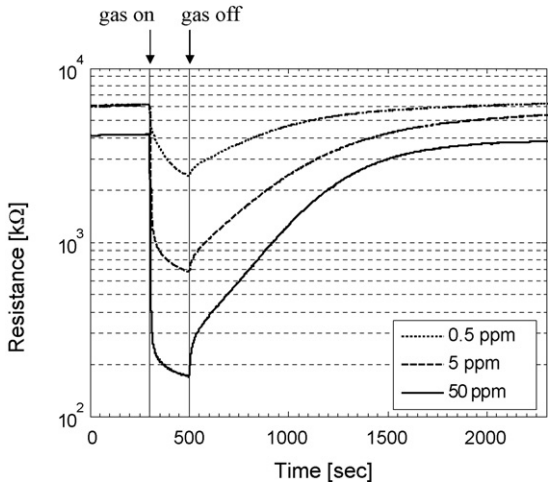

Fig. 5. Variation in the "sheet" resistance of sample A upon exposure to ethanol recorded at a layer temperature of 400 °C.

coefficients of ZnO and quartz. The preferred *c*-axis orientation found in the X-ray data of sample B can be explained by the formation of a thick film for which a texture was developed. The SEM image of sample C revealed both characteristics of samples A and B with a grain structure at the bottom of the layer and tetrapods attached on the top of the layer. The tetrapods of sample C were larger in size than those of sample A and were randomly oriented. The SEM observation and the X-ray data indicated that sample C consisted of a combination of *c*-axis oriented grains and randomly oriented tetrapods. For sample D, very little material was deposited onto the substrate, resulting in an island like structure with no texture. Poor adherence of ZnO on the quartz substrate for sample D was attributed to the absence of water. Reaction of Zn and water in an Ar flow was used to form nanostructures [4,11], but the effect of water when mixed in air on the ZnO nanotsuctures has not been studied. We concluded that water content very likely promoted the formation and the adherence onto the quartz substrates of ZnO nano/micro structures.

The three-dimensional network of tetrapods of sample A formed a highly porous structure with a high surface to volume ratio, making it an ideal candidate for use as a high-sensitivity gas sensing material. The surface to volume ratio of the fabricated samples ranked as follows: sample A > C > B.

The changes in resistance upon exposure to ethanol of samples A, B, and C were recorded using the setup of Fig. 2. Fig. 5 shows the change in resistance ('sheet resistance') of sample A operating at a temperature of 400 °C for the ethanol concentrations of 0.5, 5, and 50 ppm. It is noted that ethanol concentration as low as 0.5 ppm was easily detected. The layer response to gas is defined here as the ratio between layer resistance in air and the layer resistance in gas. The gas responses of samples A, B, and C were examined as a function of the layer temperature for a constant ethanol concentration of 50 ppm. The responses obtained for a temperature series of 200, 300 and 500 °C are plotted in Fig. 6(a). The optimum operating temperature was 400 °C for samples A and C, and 500 °C for sample B. The difference in the optimum operating temperature between the tetrapod network

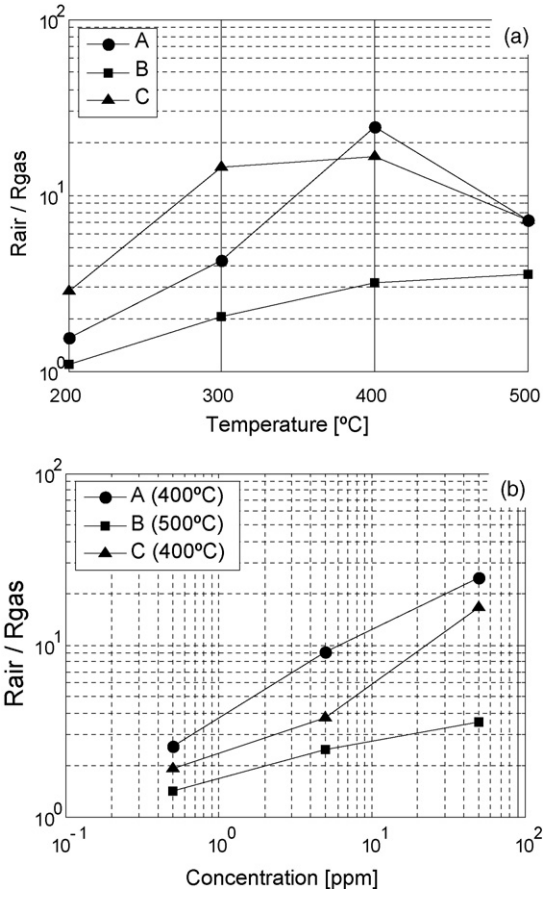

Fig. 6. Response to ethanol of the fabricated ZnO layers as a function of: (a) the operating temperature and (b) the ethanol concentration. The variations in response with the operating temperature are shown for a constant ethanol concentration of 50 ppm. The variations in response with concentration are shown for the optimum operating temperatures obtained at 50 ppm ethanol.

(sample A) and the polycrystalline film (sample B) may point to some difference in the sensing mechanisms between the tetrapod network and the polycrystalline film, the latter being known to be determined by grain boundary conductivity [17]. The gas responses of the fabricated samples recorded at the optimum layer temperature for the ethanol concentrations of 0.5, 5, and 50 ppm are shown in Fig. 6(b). The sensitivity to ethanol, as defined by the slope of the loglog response–concentration curve in Fig. 6(b), was 0.4 and 0.04 ppm^{-1} for sample A and sample B, respectively. The porous network of layer A exhibited a 10-fold increase in sensitivity when compared with the thick film of layer B. This increase in sensitivity is very likely driven by the increase in the surface-to-volume ratio of the tetrapod network structure. The gas sensing mechanism in metal oxide semiconductors relies on oxygen ion adsorption at the surface of the semiconductor and subsequent oxidation of the analyte gas by the adsorbed oxygen ions. In our n-type ZnO semiconductor [12], adsorption of oxygen ions takes electrons from the conduction band, whereas oxidation of gas molecules by adsorbed oxygen ions releases electrons. Oxygen ion adsorption and analyte gas oxidation by adsorbed oxygen ions are thus related to a decrease and an increase in carrier concentration. This gas sensing mechanism is governed by the amount of surface avail-

able for reaction, as well as the physico-chemical properties of the surface. The network of ZnO nanostructures may provide a means to drastically increase the surface available for reaction compared with those of materials in the bulk or film form. Further investigations are necessary to quantify the respective contributions of geometric characteristics and physico-chemical properties to sensitivity.

Comparison of sensor performance between different works is made difficult by the use of different measurement setups as well as different measured ranges of ethanol concentration. A rigorous comparison can only be conducted using data collected under the same experimental conditions. With this in mind, we compare our results with those reported in the literature. Responses to ethanol have been reported for two types of sensors: (1) sensors made of ZnO ceramic material [17] and (2) sensors fabricated from paste of nano/micro structured ZnO materials [10,11], for which sensitivity was computed from the published response data. Our tetrapod network (sample A) offered improvement in response by a factor 20 at 100 ppm over standard ZnO ceramic material [18]. The response values of sensors fabricated from paste of nano/micro structured powders (2 at 1 ppm for [10] and 25 at 50 ppm for [11]) were close to those of sample A. The sensitivity of our sample A was 4 times higher than that reported for the sensor element prepared from a paste of tetrapods in [11] (sensitivity estimated at $0.09\,\mathrm{ppm}^{-1}$ from their Fig. 5(a)). The use of an adhesive in the preparation of this sensor element may explain its relatively smaller sensitivity. The effect of adhesives on gas sensor responses has not been documented to our knowledge. Sample A sensitivity was 1.3 times higher than that reported for the sensor prepared from a paste of nanowires in [10] (sensitivity estimated at $0.3\,\mathrm{ppm}^{-1}$ from their Fig. 4(a) using the data in the 1–100 ppm range). It is remarkable that sample A showed a better sensitivity than a sensor prepared from nanowire powder because the surface to volume ratio of the nanowires should be higher than that of the tetrapods. This may be explained by the use of ethanol as a solvent in the preparation of the paste which likely degrades the sensor performance in detecting low concentration of ethanol. The sensitivity to ethanol of our sample A compared favorably with other sensor elements prepared from paste of powders, indicating that our sensor elements obtained by our direct fabrication process are well suited to gas detection at low concentration.

4. Conclusions

A three-dimensional network of ZnO tetrapods was fabricated on a quartz substrate via a thermal oxidation reaction. The fabrication process does not rely on the preparation of a paste from ZnO powder and its subsequent drying. The ZnO tetrapod network was deposited directly onto a quartz substrate via a thermal oxidation reaction in air from Zn powder placed in a quartz tube heated in a furnace. The morphologies of the fabricated layers were found to depend on the content of water in air. A high content of water in air promoted the growth rate forming a polycrystalline thick film, whereas no water vapor yielded almost no deposit. The tetrapod network was obtained for a small content of water of a few $\mathrm{g\,m}^{-3}$. The fabrication process did not rely on any external metal catalyst. The tetrapod network formed a highly porous structure with a high surface to volume ratio that was used as a gas sensing element. The optimum layer temperature for ethanol detection was found to be 400 °C for the tetrapod network structure and 500 °C for the polycrystalline thick film. Ethanol concentration as low as 0.5 ppm was easily detected using the tetrapod network structure at its optimum operating temperature of 400 °C. The gas sensitivity of the tetrapod network was found to be 10 times that of the thick ZnO film, pointing to superior properties of the tetrapod network over standard gas sensing elements.

References

[1] D.C. Look, Mater. Sci. Eng. B 80 (2001) 383.
[2] Ü. Özgür, Y.I. Alivov, C. Liu, A. Teke, M.A. Reshchikov, S. Dogan, V. Avrutin, S.-J. Cho, H. Morkoc, J. Appl. Phys. 98 (2005) 041301.
[3] H. Iwanaga, M. Fujii, S. Takeuchi, J. Cryst. Growth 134 (1993) 275.
[4] J.Y. Li, X.L. Chen, H. Li, M. He, Z.Y. Qiao, J. Cryst. Growth 233 (2001) 5.
[5] V.A.L. Roy, A.B. Djurisic, W.K. Chan, J. Gao, H.F. Lui, C. Surya, Appl. Phys. Lett. 83 (2003) 141.
[6] Q. Wan, C.L. Lin, X.B. Yu, T.H. Wang, Appl. Phys. Lett. 84 (2004) 124.
[7] Q. Sun, Y. Zhang, H. Chen, J. Deng, D. Wu, S. Chen, J. Catal. 167 (1997) 92.
[8] Q. Wan, T.H. Wang, J.C. Zhao, Appl. Phys. Lett. 87 (2005) 083105.
[9] Q. Wan, K. Yu, T.H. Wang, C.L. Lin, Appl. Phys. Lett. 83 (2003) 2253.
[10] Q. Wan, Q.H. Li, Y.J. Chen, T.H. Wang, X.L. He, J.P. Li, C.L. Lin, Appl. Phys. Lett. 84 (2004) 3654.
[11] C. Xiangfeng, J. Dongli, A. Djurisic, Y.H. Leung, Chem. Phys. Lett. 401 (2005) 426.
[12] J.-J. Delaunay, N. Kakoiyama, I. Yamada, SPIE 6122 (2006) (paper 612208).
[13] R.B. Heller, J. McGannon, A.H. Weber, J. Appl. Phys. 21 (1950) 1283.
[14] L. Weber, Z. Krist. 57 (1922) 398.
[15] H. Iwanaga, N. Shibata, O. Nittono, M. Kasuga, J. Cryst. Growth 45 (1978) 228.
[16] M.-S. Wu, W.-C. Shin, W.-H. Tsai, J. Phys. D 55 (1998) 943.
[17] K.-S. Weissenrieder, J. Müller, Thin Solid Films 300 (1997) 30.
[18] B. Bhooloka Rao, Mater. Chem. Phys. 64 (2000) 62.